

Where is transverse "force" in the intrinsic spin Hall effect?

Branislav K. Nikolic, Liviu P. Zăbo, and Sven Wallack

Department of Physics and Astronomy, University of Delaware, Newark, DE 19716-2570, USA

We study the spin-dependent force operator defined by the Hamiltonian of a clean quantum wire with homogeneous Rashba spin-orbit (SO) coupling attached to two ideal leads. Its expectation value in the spin-polarized electronic wave packet injected through the leads shows how the center of the packet gets deflected in the transverse direction. Moreover, the corresponding spin density will move along the transverse direction to generate an out-of-plane spin accumulation of opposite signs on the lateral edges of the wire, as expected in the phenomenology of the spin Hall effect, when spin-⁺ and spin-⁻ polarized packets (including the injection of conventional unpolarized charge current) propagate simultaneously through the ballistic semiconductor quantum wire. We also demonstrate that spin coherence of the injected spin-polarized wave packet will gradually diminish (thereby diminishing the "force") along the SO coupled wire due to entanglement of spin and orbital degrees of freedom of a single electron, even in the absence of any impurity scattering.

PACS numbers: 72.25.Dc, 71.70.Ej, 03.65.Sq

The Hall effect¹ is one of the most widely known phenomena of condensed matter physics because it represents manifestation of the fundamental concepts of electrodynamics, such as the Lorentz force, in complicated solid state environment. A perpendicular magnetic field B exerts the force $F = qv \times B$ on current flowing longitudinally along the metallic or semiconductor wire, thereby separating charges in the transverse direction which accumulate on the lateral edges of the wire. Recent optical detection^{2,3} of the accumulation of spin-⁺ and spin-⁻ electrons on the opposite lateral edges of semiconductor wires opens new realm of the spin Hall effect. This phenomenon occurs in the absence of any external magnetic fields. Instead, it requires the presence of spin-orbit couplings, which are tiny relativistic corrections that can, nevertheless, be much stronger in semiconductors than in vacuum.⁴ Besides deepening our fundamental understanding of the role of SO couplings in solids, the spin Hall effect offers new opportunities in the design of all-electrical semiconductor spintronics devices that would not require ferromagnetic elements or cumbersome e-to-control external magnetic fields.

While experimental detection of the strong signatures of the spin Hall effect brings to an end decades of theoretical speculation for its existence, it is still unclear what spin-dependent transverse "forces" are responsible for the observed spin separation. One potential mechanism, asymmetric scattering of spin-⁺ and spin-⁻ electrons off impurities with SO interaction, was invoked in the 1970s to predict the emergence of pure (i.e., not accompanied by charge transport) spin current, in the transverse direction to the flow of longitudinal unpolarized charge current, which would deposit spins of opposite signs on the lateral edges of the sample.⁵ However, it has been argued⁶ that in systems with weak SO coupling (which is unable to produce spin-splitting of the energy bands) such spin Hall effect of the extrinsic type (which vanishes in the absence of impurities) is too small to be observed with present experimental technology. Much of the recent revival of interest in the spin Hall effect has been ignited

by the predictions^{7,8} for substantially larger transverse pure spin Hall current as a response to the longitudinal electric field in semiconductors with strong SO coupling which spin-splits energy bands and induces Berry phase correction to the group velocity of Bloch wave packets.⁹ However, unusual properties of such intrinsic spin Hall current in infinite homogeneous systems, which is not conserved and depends on the whole SO coupled Fermi sea,^{7,8} have led to arguments that its non-zero value does not correspond to any real transport of spins, so that no spin accumulation near the boundaries and interfaces could be induced by intrinsic mechanisms.^{10,11}

On the other hand, mesoscopic analysis of spin-charge quantum transport through clean semiconductor wires, which is formulated in terms of genuine non-equilibrium Fermi surface quantities (conserved spin currents¹² and spin densities¹³), predicts that spin Hall accumulation^{2,3} of opposite signs on its lateral edges will emerge due to strong SO coupling within the wire region.¹³ The modeling of the spin Hall transport in experimentally accessible semiconductor structures requires to take into account the device geometry, such as its edges, interfaces, and the attached electrodes. The presence of SO couplings further emphasizes the need to treat the whole device when studying the dynamics of spin density; for example, their eigenstates^{14,15} substantially differ from the bulk ones and spin relaxation in ballistic or disordered quantum wires is highly dependent on the transverse confinement effects¹⁶ or chaotic boundaries of clean quantum dots,¹⁷ in contrast to the conventional D'yakonov-Perel' (DP) spin relaxation¹⁸ in unbounded dissipative systems where decay of spin polarization is determined solely by the SO coupling and elastic spin-independent scattering of charges on the impurities in the bulk.¹⁷

Thus, to resolve the discrepancy between different theoretical answers to such fundamental question as: Are the intrinsic¹⁹ mechanisms capable of generating the spin Hall-like accumulation on the edges of ballistic SO coupled structures? it is highly desirable to have a picture of the transverse motion of spin density in SO coupled two-

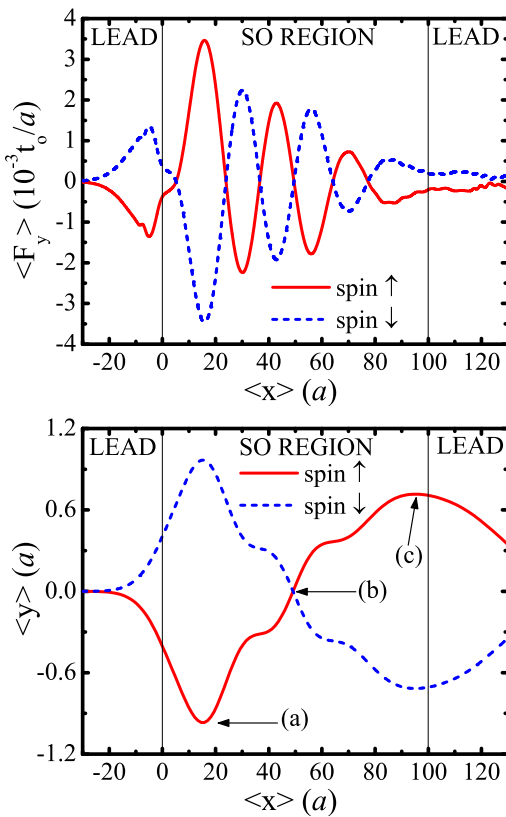


FIG. 1: The expectation value of the force operator (upper panel) and the y-coordinate of the position operator (lower panel) in the quantum state of propagating spin wave packet along the two-probe nanowire structure. The initial state in the left lead is fully spin-polarized wave packet Eq. (3), which is injected into the SO region of size $L_x = L_y = 100a = 31a$ with the Rashba coupling strength $t_{so} = 0.1t_0$ ($L_{so} = 15.7a$).

probe devices that would be as transparent as the familiar picture of transverse drift of charges due to the Lorentz force in the classical Hall effect. Here we offer such a picture by analyzing the spin-dependent transverse 'force', which can be associated with any SO coupled quantum Hamiltonian, and its effect on the semiclassical dynamics of spin density of individual electrons that are injected as spin-polarized wave packets into the Rashba SO coupled ballistic semiconductor quantum wire attached to two ideal (i.e., spin and charge interaction free) leads.

The effective mass Hamiltonian of the ballistic Rashba quantum wire is

$$\hat{H} = \frac{\hat{p}^2}{2m} + \frac{1}{\sim} (\hat{\gamma} \cdot \hat{p}) \cdot z + V_{\text{conf}}(y); \quad (1)$$

where \hat{p} is the momentum operator in 2D space, $\hat{\gamma} = (\hat{\gamma}^x, \hat{\gamma}^y, \hat{\gamma}^z)$ is the vector of the Pauli spin operators, and $V_{\text{conf}}(y)$ is the transverse potential confining electrons to a wire of finite width. We assume that the wire of dimensions $L_x = L_y$ is realized using the two-dimensional electron gas (2D EG), with z being the unit vector orthogonal to its plane. Within the 2D EG carriers are sub-

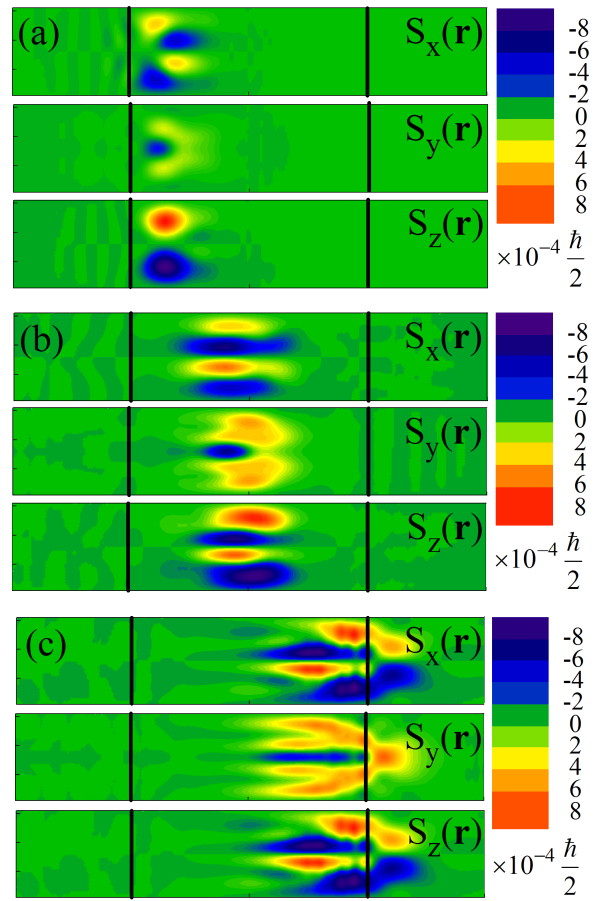


FIG. 2: The dynamics of spin density ($S_x(r)$, $S_y(r)$, $S_z(r)$) induced by simultaneous propagation of two electrons through quantum wire $100a = 31a$ with the Rashba SO coupling $t_{so} = 0.1t_0$. Both electrons are injected at $t = 0$ from the left lead, one as spin-'-' and the other one as spin-'+' polarized (along the z-axis) wave packet Eq. (3). The different snapshots of the sum of their spin densities are taken at the points where the 'force' and the y-coordinate of the center of such wave packets have values shown in Fig. 1.

jected to the Rashba SO coupling of strength t_{so} , which arises due to structure inversion asymmetry⁴ (of the conning potential and di ering band discontinuities at the heterostructure quantum well interface²⁰). This Hamiltonian generates spin-dependent force operator that can be extracted^{21,22} within the Heisenberg picture²³ as

$$\begin{aligned} \hat{F}_H &= m \frac{d\hat{r}_H^2}{dt^2} = \frac{m}{\sim^2} [\hat{p}_H; \hat{H}]; \hat{H}] \quad (2) \\ &= \frac{2^2 m}{\sim^3} (\hat{p}_H - z) \cdot \hat{\gamma}_H^z \frac{dV_{\text{conf}}(\hat{y}_H)}{dy_H} y: \end{aligned}$$

Here the Heisenberg picture operators carry the time dependence of quantum evolution, i.e., $\hat{p}_H(t) = e^{i\hat{H}t} \hat{p} e^{-i\hat{H}t}$, $\hat{\gamma}_H^z(t) = e^{i\hat{H}t} \hat{\gamma}^z e^{-i\hat{H}t}$, and $\hat{y}_H(t) = e^{i\hat{H}t} \hat{y} e^{-i\hat{H}t}$, where $\hat{\gamma}^z$, \hat{p} , and \hat{y} are in the Schrodinger picture and, therefore, time-independent.

Since the force operator²² depends on spin through

\hat{F}_y^z , which is a genuine (internal) quantum degree of freedom,²³ it does not have any classical analog. Its physical meaning (i.e., measurable prediction) is contained in the expectation value $\hat{h}F_y^z i(t) = h(t=0)j\hat{F}_y^z(t)j(t=0)i$, obtained by acting with force operator on a quantum state $j(t=0)i$ of an electron. While such "force" can always be derived from a given quantum Hamiltonian, its usefulness in understanding the evolution of quantum systems is limited by the local nature of the force equation cannot be reconciled with inherent non-locality of quantum mechanics. For example, if the force "pushes" the volume of a wave function locally, one has to find a new global wave function in accord with the boundary conditions at infinity (the same problem remains well-hidden in the Heisenberg picture where time dependence is carried by the operators while wave functions are time-independent). Nevertheless, analyzing the dynamics of spin and probability densities in terms of the action of local forces can be insightful for particles described by wave packets (whose probability distribution is small compared to the typical length scale over which the force varies).²³

Therefore, we examine in Fig. 1 the transverse "force" $\hat{h}F_y^z i$ in the spin wave packet state, which at $t=0$ resides in the left lead as fully spin-polarized (along the z -axis) and localized wave function^{14,24}

$$(t=0) = C \sin \frac{y}{(L_y + 1)a} e^{ik_x x - k_x^2 x^2/4} \quad : (3)$$

This is a pure and separable $j(t=0)i = j_i j_i$ quantum state in the tensor product of the orbital and spin Hilbert spaces $H_o \otimes H_s$. The orbital factor state $h_x; y j_i$ consists of the lowest subband of the hard wall transverse conning potential and a Gaussian wave packet along the x -axis whose parameters are $k_x a = 0.44$ and $k_y a = 0.1$ (C is the normalization constant $h_j i = 1$). The spin factor state is an eigenstate of \hat{z} , i.e., $\hat{z} = \begin{pmatrix} 0 \\ 1 \end{pmatrix}$ or

$$\hat{z} = \begin{pmatrix} 0 \\ 1 \end{pmatrix}. \quad \text{Unlike the case}^{21} \text{ of an infinite 2DEG,}$$

the exact solutions of the Heisenberg equation of motion for $\hat{z}_H^z(t)$, $\hat{y}_H^z(t)$ and $\hat{p}_H^z(t)$ entering in Eq. (2) are not available for quantum wires of finite width. Thus, we compute the expectation value $h(t)j\hat{F}_y^z j(t)i$ in the Schrödinger picture by applying the evolution operators $e^{i\hat{H}^z t}$ present in Eq. (2) on the wave functions $j(t)i = \sum_n e^{iE_n t} j_n i$ and eigenvalues E_n , we employ the discretized version of the Hamiltonian Eq. (1). That is, we represent the Hamiltonian of the Rashba spin-split quantum wire in the basis of states $j_m i = j_i$, where $j_m i$ are s-orbitals $h_r j_m i = (r_m)$ located at sites $m = (m_x, m_y)$ of the $L_x \times L_y$ lattice with the lattice spacing a (typically¹⁶ $a = 3 \text{ nm}$). This representation extracts the two energy scales from the Rashba Hamiltonian Eq. (1): $t_o = \hbar^2/(2m a^2)$ characterizing hopping between the nearest-neighbor sites without spin- \hat{p} ; and $t_{so} = -2a$ for the same hopping process when it involves

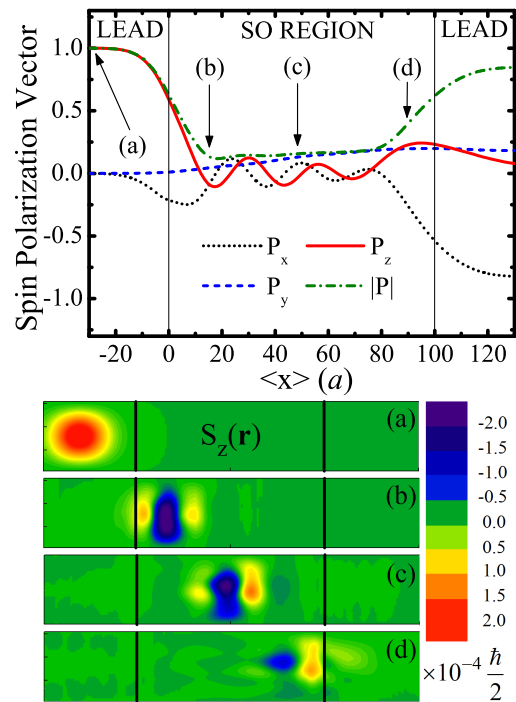


FIG. 3: Spin precession, as signified by oscillations of the spin polarization vector ($P_x; P_y; P_z$), and spin decoherence (as measured by decrease of the purity \mathcal{P} below one) of the spin state of a single electron propagating along the Rashba quantum wire $100a \times 31a$ with the SO coupling strength $t_{so} = 0.1t_o$ ($L_{so} = 15.7a$). The electron is injected from the left lead as a spin- $\frac{1}{2}$ polarized wave packet, whose spin subsystem is therefore fully coherent $\mathcal{P} = 1$ at $t = 0$. The bottom panel shows the z -component of the spin density $S_z(r)$ at different values of $\frac{1}{2}P_z = -dr S_z(r)$ along the wire.

spin \hat{p} .^{13,16} The wave vector of the Gaussian packet $k_x a = 0.44$ is chosen¹³ to correspond to the Fermi energy $E_F = 3.8t_o$ close to the bottom of the band where tight-binding dispersion relation reduces to the parabolic one of the Hamiltonian Eq. (1). In this representation one can directly compute the commutators in the definition of the force operator Eq. (2), thereby bypassing subtleties which arise when evaluating the transverse component of the force operator $dV_{\text{conf}}(\hat{y}_H^z)j = d\hat{y}_H^z$ stemming from the hard wall boundary conditions.²⁸

Figure 1 shows that as soon as the front of the spin-polarized wave packet enters the SO region, its center $h\hat{y}_H^z i(t) = h(t)\hat{y}_H^z i$ will be deflected along the y -axis in the same direction as is the direction of the "force". However, due to its inertia the packet does not follow fast oscillations of the "force" occurring on the scale set by the spin precession length^{13,16} $L_{so} = t_o/2t_{so}$ (on which spin precess by an angle π). In contrast to the infinite 2DEG of macroscopic studies of the intrinsic spin Hall effect,^{8,10,11} in ballistic quantum wires electron motion is confined in the transverse direction and the effective momentum-dependent Rashba magnetic field $B_R(k)$ is, therefore, parallel to this direction¹⁵ (or nearly parallel in

disordered wires¹⁶). Thus, the change of the direction of the transverse spin-dependent "force" is due to the fact that the z-axis is polarized spin will start precessing within the SO region since it is not an eigenstate of the Zeeman term $\hat{B}_R(k)$ [i.e., the Rashba term in Eq. (1)].

The transverse spin-dependent "force" and the motion of the center of the wave packet in Fig. 1 suggests that when two electrons of opposite spin-polarization are injected simultaneously into the SO coupled quantum wire with perfectly homogeneous²⁴ Rashba coupling, the initially unpolarized mixed spin state will evolve during propagation through the wire to develop a non-zero spin density at its lateraledges. This intuitive picture is confirmed by plotting in Fig. 2 the spin density, $S_m(t) = \frac{1}{2}h(t)\hat{j}^\dagger \sin \theta \sin \phi = \frac{1}{2}c_m^+ c_m^- h^\dagger \hat{j}^\dagger$, corresponding to coherent evolution of two spin wave packets, $j(t=0) = j^+ + j^-$ and $j(t=0) = j^+ - j^-$, through the wire.

The mechanism underlying the decay of the transverse "force" intensity is explained in Fig. 3, where we demonstrate that (initially coherent) spin precession is also accompanied by spin decoherence.¹⁶ These two processes are encoded in the rotation of the spin polarization vector P and the reduction of its magnitude ($\hat{P} j = 1$ for fully coherent pure states $\hat{s}^2 = \hat{s}$), respectively. The spin polarization vector determines the density matrix $\hat{s} = (1 + P^\dagger) = 2$ of the spin subsystem,²³ which is obtained by tracing the pure state density matrix $\hat{\rho}(t) = j(t)ih(t)j^\dagger$ over the orbital degrees of freedom at each instant of time, $\hat{s}(t) = \text{Tr}_0 j(t)ih(t)j^\dagger = \frac{1}{2}h(t)\hat{j}^\dagger \sin \theta \sin \phi = \frac{1}{2}c_m^+ c_m^- h^\dagger \hat{j}^\dagger$. Note that dynamics of the spin polarization vector and the spin density shown in Fig. 3 are in one-to-one correspondence, $\frac{1}{2}P(t) = \frac{1}{2}S_m(t)$. The incoming quantum state from the left lead in Fig. 3 is separable $j(t=0) = j^+ + j^-$, and therefore fully spin coherent $\hat{P} j = 1$. However, in the course of propagation through SO coupled quantum wires with many subbands it will coherently evolve into a non-separable²³ state where spin and orbital subsystems of the same electron appear to be entangled.^{16,25}

While this process is analogous to the well-known DP spin relaxation in disusive SO coupled systems,¹⁸ here the decay of spin polarization vector takes place without any scattering on impurities. Instead, it arises due to the presence of interfaces¹⁶ (the wave packet is partially reflected at the lead/SO-region interface for strong Rashba coupling) and boundaries^{16,17} of the confined structure. Thus, the spin decoherence mechanism revealed in Fig. 3 is highly relevant for the interpretation of experiments on the transport of spin coherence in high-mobility semiconductors²⁶ and molecular spintronic devices.²⁷

The interplay of the oscillating and decaying (induced by spin precession and spin decoherence, respectively) transverse spin-dependent "force" and wave packet inertia is that spin- \uparrow electron will exit the wire with its center and the corresponding spin- \uparrow density deected toward the left lateral edge.¹³ This picture is only apparently

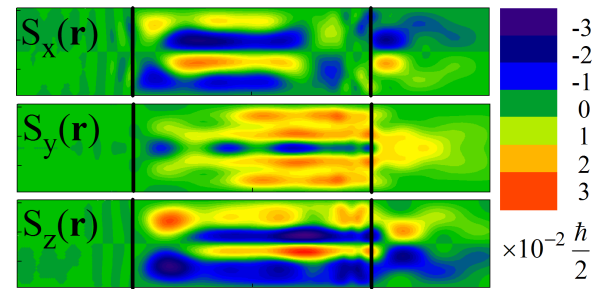


FIG. 4: The spin accumulation ($S_x(r)$, $S_y(r)$, $S_z(r)$) induced by the ballistic flow of unpolarized charge current, simulated by injecting one after another 150 pairs of spin- \uparrow and spin- \downarrow polarized (along the z-axis) wave packets from the left lead, through quantum wire 100a 31a with the Rashba SO coupling $t_{so} = 0.1t_0$.

counterintuitive to the naive conclusion drawn from the form of the force operator Eq. (2), suggesting that spin- \uparrow electron is deected to the right while moving along the Rashba SO region (as happens clearly only at the entrance into the SO region in Fig. 1), since one has to take into account the ratio $L_{so} = L_x$.

Moreover, when we inject pairs of spin- \uparrow and spin- \downarrow polarized wave packets one after another, thereby simulating the flow of unpolarized ballistic current through the lead-wire-lead structure (where electron does not feel any electric field within the clean quantum wire region),¹³ we find in Fig. 4 that the deection of the spin densities of individual electrons in the transverse direction will generate non-zero spin accumulation components $S_z(r)$ and $S_x(r)$ of the opposite sign on the lateraledges of the wire. While recent experiments find $S_z(r)$ with such properties to be the strong signature of the spin Halle effect,^{2,3} here we confirm our conjecture of Ref. 13 that $S_x(r)$ is also a feature of the spin Halle effect, it arises due to the precession (Fig. 3) of transversally deected spins.

In conclusion, the spin-dependent force operator, defined by the SO coupling terms of the Hamiltonian of a ballistic spin-split semiconductor quantum wire, will act on the injected spin-polarized wave packets to deect spin- \uparrow and spin- \downarrow electrons in the opposite transverse directions. This effect, combined with precession and decoherence of the deected spin, will lead to non-zero z- and x-components of the spin density with opposite signs on the lateral edges of the wire, as expected from the spin Halle effect phenomenology^{5,13} and confirmed in recent experiments.^{2,3} The intuitively appealing picture of the transverse "force" (as a counterpart of the classical Lorentz force), which depends on spin through \hat{z}^2 , the strength of the Rashba SO coupling through \hat{z}^2 , and the momentum through the cross product $\hat{p} \cdot \hat{z}$, allows one to differentiate symmetry properties of the two spin Hall accumulation components upon changing the Rashba electric field (i.e., the sign of \hat{z}) or the direction of the packet propagation: $S_z(r) = S_z(r)$ and $S_z(r)_p = -S_z(r)_p$ vs. $S_x(r) = -S_x(r)$ (due to opposite spin precession

for $S_x(r)$ and $S_x(r)_p = S_x(r)p$. These features are in full accord with experimentally observed behavior of the intrinsic spin Hall accumulation under the inversion of the bias voltage,³ as well as with the formal quantum transport analysis¹³ of the non-equilibrium spin accumulation.

lation induced by the flow of unpolarized current through ballistic SO coupled two-probe nanostructures.

We are grateful to S. Souma for insightful discussions. This work was supported in part by ACS grant No. PRF-41331-G 10.

Present address: Institut für Physik, Technische Universität, D-09107 Chemnitz, Germany

- ¹ The Hall Effect and its Applications, edited by C. L. Chien and C. W. Westgate (Plenum, New York, 1980).
- ² Y. K. Kato, R. C. Myers, A. C. Gossard, and D. D. Awschalom, *Science* **306**, 1910 (2004).
- ³ J. Wunderlich, B. Kaestner, J. Sinova, and T. Jungwirth, *Phys. Rev. Lett.* **94**, 047204 (2005).
- ⁴ E. I. Rashba, *Physica E* **20**, 189 (2004).
- ⁵ M. I. D'yakonov and V. I. Perel', *JETP Lett.* **13**, 467 (1971); J. E. Hirsch, *Phys. Rev. Lett.* **83**, 1834 (1999); S. Zhang, *Phys. Rev. Lett.* **85**, 393 (2000).
- ⁶ B. A. Bernevig and S.-C. Zhang, cond-mat/0412550.
- ⁷ S. Murakami, N. Nagaosa, and S.-C. Zhang, *Science* **301**, 1348 (2003); *Phys. Rev. B* **69**, 235206 (2004).
- ⁸ J. Sinova et al., *Phys. Rev. Lett.* **92**, 126603 (2004).
- ⁹ D. Culcer et al., *Phys. Rev. Lett.* **93**, 046602 (2004); G. Sundaram and Q. Niu, *Phys. Rev. B* **59**, 14195 (1999).
- ¹⁰ E. I. Rashba, *Phys. Rev. B* **70**, 161201(R) (2004); **68**, 241315(R) (2003).
- ¹¹ S. Zhang and Z. Yang, *Phys. Rev. Lett.* **94**, 066602 (2005).
- ¹² S. Souma and B. K. Nikolic, cond-mat/0410716 (to appear in *Phys. Rev. Lett.*).
- ¹³ B. K. Nikolic, S. Souma, L. P. Zárbo, and J. Sinova, cond-mat/0412595.
- ¹⁴ M. Valin-Rodríguez, A. Puente, and L. Serra, *Eur. Phys. J. B* **34**, 359 (2003).
- ¹⁵ M. Goveas and U. Zulicke, *Phys. Rev. B* **66**, 073311 (2002); cond-mat/0407036.

- ¹⁶ B. K. Nikolic and S. Souma, cond-mat/0402662.
- ¹⁷ C.-H. Chang, A. G. M. al'shukov, and K. A. Chao, *Phys. Rev. B* **70**, 245309 (2004).
- ¹⁸ M. I. D'yakonov and V. I. Perel', *Fiz. Tverd Tela* **13**, 3581 (1971) [Sov. Phys. Solid State **13**, 3023 (1972)]; *Zh. Eksp. Teor. Fiz.* **60**, 1954 (1971) [Sov. Phys. JETP **33**, 1053 (1971)].
- ¹⁹ To avoid possible confusion with the bulk studies (where "intrinsic"^{7,8,11} is used to denote spin Hall current arising from the equilibrium distribution function and spin-split band structure due to the SO coupling), here we use the term "intrinsic" for any mechanism which leads to spin-Hall-type effect^{2,3} in ballistic SO coupled devices.
- ²⁰ P. Pfeifer, *Phys. Rev. B* **59**, 15902 (1998).
- ²¹ J. Schliemann, D. Loss, and R. Westervelt, cond-mat/04010321.
- ²² J. Li, L. Hu, and S.-Q. Shen, cond-mat/0502102.
- ²³ L. E. Ballentine, *Quantum Mechanics: A Modern Development* (World Scientific, Singapore, 1998).
- ²⁴ J. I. Ohe, M. Yamamoto, T. Ohtsuki, and J. Nitta, cond-mat/0409161;
- ²⁵ A. Peres and D. R. Terno, *Rev. Mod. Phys.* **76**, 93 (2004).
- ²⁶ J. M. Kikkawa and D. D. Awschalom, *Nature* (London) **397**, 139 (1999).
- ²⁷ B. W. Apfelaar, K. T. Suzuki, and M. Wagner, *J. of Appl. Phys.* **89**, 6863 (2001).
- ²⁸ D. S. Rokhsar, *Am. J. Phys.* **64**, 1416 (1996).